Research Article | Vol. 6, No. 10 | 1 Oct 2016 | OPTICAL MATERIALS EXPRESS 3063

Optical Materials EXPRESS

Efficient photoinduced charge transfer in chemically-linked organic-metal Ag-P3HT nanocomposites

LIN FENG,[1] MING CHEN,[1,5] FEI ZHENG,[1] MENG-SI NIU,[1] XUEHUA ZHANG,[2,3] XIAO-TAO HAO[1,4,6]

[1]*School of Physics, State Key Laboratory of Crystal Materials, Shandong University, Jinan, Shandong, 250100 China*
[2]*Soft Matter and Interfaces Group, School of Engineering, RMIT University, Melbourne, VIC 3001, Australia*
[3]*Physics of Fluids Group, Department of Science and Technology, J. M. Burgers Center for Fluid Dynamics, and Mesa + Institute, University of Twente, 7500 AE Enschede, The Netherlands*
[4]*School of Chemistry, The University of Melbourne, Parkville, Victoria 3010, Australia*
[5]*chenming@sdu.edu.cn*
[6]*haoxt@sdu.edu.cn*

Abstract: A novel nanocomposite of P3HT and Ag nanoparticles (Ag-P3HT) has been synthesized by laser ablation. The fluorescence wavelength of the nanocomposite can be tuned by varying the ablation duration. The steady-state emission maximum at 580 nm for pristine P3HT shows significant blueshift to wavelengths ranging from 520 to 550 nm for Ag-P3HT. NMR, FTIR and XPS spectroscopy confirm that chemical links are formed between P3HT and silver nanoparticles (NPs) in the nanocomposite. For the sample with an emission maximum at 530 nm, ^{1}H NMR spectra indicate that 66% of the P3HT thiophene ring protons are replaced by Ag NPs. Time-resolved spectroscopy demonstrates that charge transfer efficiency increases for Ag-P3HT and this is attributed to the enhanced intimate interfacial contact between the chemically-bonded metal NPs and polymer chains. The synthetic route outlined provides a one-pot and green strategy for producing metal-organic polymeric materials, with controlled luminescence wavelengths and efficient photoinduced charge transfer that meet the requirement for developing high-performance organic light-emitting and photovoltaic devices.

OCIS codes: (160.2540) Fluorescent and luminescent materials; (160.5470) Polymers.

References and links

1. S. Ren, L. Y. Chang, S. K. Lim, J. Zhao, M. Smith, N. Zhao, V. Bulović, M. Bawendi, and S. Gradecak, "Inorganic-organic hybrid solar cell: bridging quantum dots to conjugated polymer nanowires," Nano Lett. **11**(9), 3998–4002 (2011).
2. G. W. Gokel, W. M. Leevy, and M. E. Weber, "Crown ethers: sensors for ions and molecular scaffolds for materials and biological models," Chem. Rev. **104**(5), 2723–2750 (2004).
3. C. P. Ponce, R. P. Steer, and M. F. Paige, "Photophysics and halide quenching of a cationic metalloporphyrin in water," Photochem. Photobiol. Sci. **12**(6), 1079–1085 (2013).
4. Y. Cui, Y. Yue, G. Qian, and B. Chen, "Luminescent functional metal-organic frameworks," Chem. Rev. **112**(2), 1126–1162 (2012).
5. T. Erb, U. Zhokhavets, G. Gobsch, S. Raleva, B. Stuhn, P. Schilinsky, C. Waldauf, and C. J. Brabec, "Correlation between structural and optical properties of composite polymer/fullerene films for organic solar cells," Adv. Funct. Mater. **15**(7), 1193–1196 (2005).
6. T. Segal-Peretz, O. Sorias, M. Moshonov, I. Deckman, M. Orenstein, and G. L. Frey, "Plasmonic nanoparticle incorporation into inverted hybrid organic–inorganic solar cells," Org. Electron. **23**(2), 144–150 (2015).
7. L. Zhao, X. Pang, R. Adhikary, J. W. Petrich, and Z. Lin, "Semiconductor anisotropic nanocomposites obtained by directly coupling conjugated polymers with quantum rods," Angew. Chem. Int. Ed. Engl. **50**(17), 3958–3962 (2011).
8. T. Xu, M. Yan, J. D. Hoefelmeyer, and Q. Qiao, "Exciton migration and charge transfer in chemically linked P3HT-TiO_2 nanorod composite," RSC Advances **2**(3), 854–862 (2012).

#272713 http://dx.doi.org/10.1364/OME.6.003063
Journal © 2016 Received 29 Jul 2016; revised 30 Aug 2016; accepted 1 Sep 2016; published 8 Sep 2016

Optical Materials EXPRESS

9. D. Lee and D. J. Jang, "Charge-carrier relaxation dynamics of poly(3-hexylthiophene)-coated gold hybrid nanoparticles," Polymer (Guildf.) **55**(21), 5469–5476 (2014).
10. J. Fujisawa and M. Hanaya, "Extremely strong organic-metal oxide electronic coupling caused by nucleophilic addition reaction," Phys. Chem. Chem. Phys. **17**(25), 16285–16293 (2015).
11. Z. Lin, "Organic-inorganic nanohybrids through the direct tailoring of semiconductor nanocrystals with conjugated polymers," Chemistry **14**(21), 6294–6301 (2008).
12. P. Sista, K. Ghosh, J. S. Martinez, and R. C. Rocha, "Metallo-biopolymers: conjugation strategies and applications," Polym. Rev. (Phila. Pa.) **54**(4), 627–676 (2014).
13. K. W. Lo, P. K. Lee, and S. Y. Lau, "Synthesis, characterization, and properties of luminescent organoiridium(III) polypyridine complexes appended with an alkyl chain and their interactions with lipid bilayers, surfactants, and living cells," Organometallics **27**(13), 2998–3006 (2008).
14. S. Li, D. M. Wang, Z. Y. Wang, Z. W. Wang, M. Chen, and X. D. Liu, "Laser-induced fabrication of single crystal zinc hydroxyl dodecyl sulfate nano-sheets with excellent fluorescence emission," RSC Advances **5**(78), 63233–63239 (2015).
15. Y. Y. Lin, Y. Y. Lee, L. Chang, J. J. Wu, and C. W. Chen, "The influence of interface modifier on the performance of nanostructured ZnO/polymer hybrid solar cells," Appl. Phys. Lett. **94**(6), 063308 (2009).
16. M. A. H. Muhammed, F. Aldeek, G. Palui, L. Trapiella-Alfonso, and H. Mattoussi, "Growth of in situ functionalized luminescent silver nanoclusters by direct reduction and size focusing," ACS Nano **6**(10), 8950–8961 (2012).
17. M. R. Kern and S. G. Boyes, "Raft polymerization kinetics and polymer characterization of P3HT rod-coil block copolymers," J. Polym. Sci. Pol. Chem. **52**(24), 3575–3585 (2014).
18. F. Alam, N. Kumar, and V. Dutta, "Study of surfactant-free lead sulfide nanocrystals-P3HT hybrid polymer solar cells," Org. Electron. **22**, 44–50 (2015).
19. T. A. Chen, X. Wu, and R. D. Rieke, "Region controlled synthesis of poly(3-alkylthiophenes) mediated by riekezinc: their characterization and solid-state properties," J. Am. Chem. Soc. **117**(1), 233–244 (1995).
20. B. Ferreira, P. F. da Silva, J. S. Seixas de Melo, J. Pina, and A. Maçanita, "Excited-state dynamics and self-organization of poly(3-hexylthiophene) (P3HT) in solution and thin films," J. Phys. Chem. B **116**(8), 2347–2355 (2012).
21. J. Xiao, Q. Yue, B. Gao, Y. Sun, J. Kong, Y. Gao, Q. Li, and Y. Wang, "Performance of activated carbon/nanoscale zero valent iron for removal of trihalomethanes (THMs) at infinitesimal concentration in drinking water," Chem. Eng. J. **253**(1), 63–72 (2014).
22. C. J. Lee, M. R. Karim, and S. L. Mu, "Synthesis and characterization of silver/thiophene nanocomposites by UV-irradiation method," Mater. Lett. **61**(13), 2675–2678 (2007).
23. P. Yu, X. M. Wen, Y. R. Toh, X. Q. Ma, and J. Tang, "Fluorescent metallic nanoclusters: electron dynamics, structure, and applications," Part. Part. Syst. Charact. **32**(2), 142–163 (2015).
24. D. Lee and D. J. Jang, "Charge-carrier relaxation dynamics of poly(3-hexylthiophene)-coated gold hybrid nanoparticles," Polymer (Guildf.) **55**(21), 5469–5476 (2014).
25. S. Maensiri, C. Masingboon, V. Promarak, and S. Seraphin, "Synthesis and optical properties of nanocrystalline V-doped ZnO powders," Opt. Mater. **29**(12), 1700–1705 (2007).
26. C. Taliani and L. M. Blinov, "The electronic structure of solid αsexithiophene," Adv. Mater. **8**(4), 353–359 (1996).
27. M. Baghgar, J. A. Labastide, F. Bokel, R. C. Hayward, and M. D. Barnes, "Effect of polymer chain folding on the transition from H- to J-aggregate behavior in P3HT nanofibers," J. Phys. Chem. C **118**(4), 2229–2235 (2014).
28. F. Zheng, W. L. Xu, H. D. Jin, M. Q. Zhu, W. H. Yuan, X. T. Hao, and K. P. Ghiggino, "Purified dispersions of graphene in a nonpolar solvent via solvothermal reduction of graphene oxide," Chem. Commun. (Camb.) **51**(18), 3824–3827 (2015).
29. P. J. Brown, D. S. Thomas, A. Kohler, J. S. Wilson, J. S. Kim, C. M. Ramsdale, H. Sirringhaus, and R. H. Friend, "Effect of interchain interactions on the absorption and emission of poly(3-hexylthiophene)," Phys. Rev. B **67**(6), 480–485 (2003).
30. H. Ohkita, S. Cook, Y. Astuti, W. Duffy, S. Tierney, W. Zhang, M. Heeney, I. McCulloch, J. Nelson, D. D. Bradley, and J. R. Durrant, "Charge carrier formation in polythiophene/fullerene blend films studied by transient absorption spectroscopy," J. Am. Chem. Soc. **130**(10), 3030–3042 (2008).
31. W. L. Xu, B. Wu, F. Zheng, H. B. Wang, Y. Z. Wang, F. G. Bian, X.-T. Hao, and F. Zhu, "Homogeneous phase separation in polymer:fullerene bulk heterojunction organic solar cells," Org. Electron. **25**, 266–274 (2015).
32. M. Hufnagel, M. Fischer, T. Thurn-Albrecht, and M. Thelakkat, "Influence of fullerene grafting density on structure, dynamics, and charge transport in P3HT-b-$PPC_{61}BM$ block copolymers," Macromolecules **49**(5), 1637–1647 (2016).
33. I. W. Hwang, D. Moses, and A. J. Heeger, "Photoinduced carrier generation in P3HT/PCBM bulk heterojunction materials," J. Phys. Chem. C **112**(11), 4350–4354 (2008).
34. J. L. Wu, F. C. Chen, Y. S. Hsiao, F. C. Chien, P. Chen, C. H. Kuo, M. H. Huang, and C. S. Hsu, "Surface plasmonic effects of metallic nanoparticles on the performance of polymer bulk heterojunction solar cells," ACS Nano **5**(2), 959–967 (2011).

Optical Materials EXPRESS

35. G. J. Hedley, A. J. Ward, A. Alekseev, C. T. Howells, E. R. Martins, L. A. Serrano, G. Cooke, A. Ruseckas, and I. D. Samuel, "Determining the optimum morphology in high-performance polymer-fullerene organic photovoltaic cells," Nat. Commun. **4**, 2867 (2013).

1. Introduction

Metal-organic luminescent materials have been extensively investigated and applied in lighting, display, sensing, and optical devices [1–3]. Metal-polymers integrate the optical, electronic, magnetic, and chemical properties of metal complexes with the specificity and highly ordered structures of polymers [4,5].

Poly(3-hexylthiophene) (P3HT) is a conjugated polymer that is often used in organic light-emitting and photovoltaic devices. P3HT fluoresces over a broad range (500-900 nm) and its absorption and emission arise from π-π* transitions associated with the conjugated thiophene rings. The bandgap and the luminescence wavelength can be manipulated by chemically linking the thiophene moieties to metals or other semiconductor components, often facilitating the migration and dissociation of excitons and promoting photovoltaic performance.

In most previous studies, metal nanoparticles (NPs) were merely physically mixed with P3HT to enhance the free charge transfer [6]. In the resulting mixture, the charge transfer between P3HT and the metal is hindered by the insulating medium as well as the strong phase segregation associated with physical mixing. Several research groups reported that inorganic NPs or nanorods (NRs) could be chemically-grafted to P3HT, showing improvements in terms of generation efficiency of free charge carriers [7–9]. However, up to now, only pre-modified P3HT (e.g. SH- or vinyl- terminated P3HT) has been used in all the functionalization by chemically grafting. The chemically bonded NPs are thus rather isolated from the main chain and the fluorescence of P3HT has not been affected. To the best of our knowledge, incorporation of the metal into the thiophene ring moiety of P3HT to produce complex nanocomposite has not been explored to date.

To incorporate metal NPs into the organic polymers, there are a multitude of synthetic methodologies available [10–12]. Among them, the conventional synthetic strategies are either ligand exchange or using coupling chemicals to combine metal to polymers under hydrothermal conditions [10,11]. Catalysts or surfactants are usually required to implement the reaction [12,13], and multiple steps involved in the process are time consuming. As an attractive technique characterized by non-equilibrium phase change, laser ablation fabrication in liquids is a rapidly-developing green approach, which does not require an intermediate workup process or any potentially toxic catalyst [14,15].

When a laser beam is focused on the surface of a silver target immersed in a solution, the super-heating plays a critical role in the early stage (0-20 ns), resulting in excited Ag ions. Due to the Ag plasma expansion, a shock wave is emitted, followed by a cavitation bubble formation, expansion and collapse [14,15]. During pulses of laser-induced Ag plasma in the liquid, the excited Ag ions are reactive, offering a highly promising approach to produce metal nanostructures in a simple and controllable process [14].

In this work, we present an efficient and convenient route based on laser ablation to chemically link neat P3HT to silver NPs, forming a novel organic-metal Ag-P3HT complex nanocomposite. The aim is to achieve tunable luminescence of Ag-P3HT via chemically tethering metal NPs to the thiophene ring of P3HT. During the laser ablation process, the laser induced Ag plasma associated with high pressure and temperature in local domains, promotes the reaction of Ag ions with P3HT [14,15]. In 30 min, a novel nanocomposite, Ag-P3HT, can be successfully prepared. The structure of the novel nanocomposite was confirmed by ^{1}H NMR, FTIR and XPS techniques. The nanocomposites exhibit tunable luminescence and improved charge transfer efficiency.

Thanks to the chemical bond between Ag and P3HT, the as-prepared Ag-P3HT shows a strong blueshift in the steady-state absorption and photoluminescence (PL)spectra. Time-resolved fluorescence spectroscopy shows chemically-bonded Ag-P3HT is superior to

Optical Materials EXPRESS

pristine P3HT and physically-mixed Ag/P3HT in terms of exciton dissociation and charge carrier migration.

2. Experimental

P3HT (Poly(3-hexylthiophene-2,5-diyl), >90% region regular, average molecule weight: 60k) was purchased from Sigma-Aldrich and dissolved in chloroform at a concentration of 0.5mg/ml. P3HT solutions were stirred overnight. During the laser ablation process, a well-polished pure (99.99%) Ag target was placed on the bottom of a glass bottle filled with the P3HT solution. A Q-switched Nd-YAG laser (Quanta Ray, SpectraPhysics) operates at a wavelength of 1064 nm with a pulse duration of 10 ns and repetition rate of 10 Hz. The laser beam was focused onto the target by a quartz lens with a focal length of 45 mm and the average laser spot size at the target was measured to be 1mm. The laser beam intensity was about 6 $GWcm^{-2}$ and the ablation lasted for 15/30/40/50 min [15].

Subsequently the nanocomposite of Ag and P3HT was characterized using ^{1}H NMR spectra which were acquired in deuterochloroform ($CDCl_3$) on a Bruker DMX-300 nuclear resonance spectrometer. High-resolution transmission electron microscopy (HRTEM) images were obtained with a JEOL JEM-3000F microscope. The samples were prepared by dropping dilute solutions onto carbon-coated copper grids and the solvent was allowed to evaporate in air. Fourier-transform infrared (FTIR) spectra were obtained at room temperature in the transmittance mode using a Bruker ALPHA-T infrared spectrometer within the wavenumber range of 400-2000 cm^{-1} at a resolution of 1.43 cm^{-1}. XPS was characterized on an X-ray photoelectron spectrometer (ESCALAB250, Thermo Fisher SCIENTIFIC) with a pressure $<10^{-7}$ Pa.

The optical absorption spectra were collected using a UV-visible dual-beam spectrophotometer (UV-1800, Shimadzu). Steady-state PL measurements were carried out using a PG2000-Pro-EX spectrometer with an excitation wavelength of 400 nm. Time-resolved fluorescence characterization was performed using the time-correlated single-photon-counting (TCSPC) technique [16]. The excitation wavelength is 400 nm from the second harmonic output of a Ti: sapphire laser (Maitai HP, Spectra-Physics) at 80 MHz. The time-resolved PL data were collected by a Halcyone spectrometer (Ultrafast System). The measurement error of the spectrometer is about ± 25 ps. The data were fitted using exponential convolution methods.

Optical Materials EXPRESS

3. Results and discussion

Emission tuning and morphology of Ag-P3HT

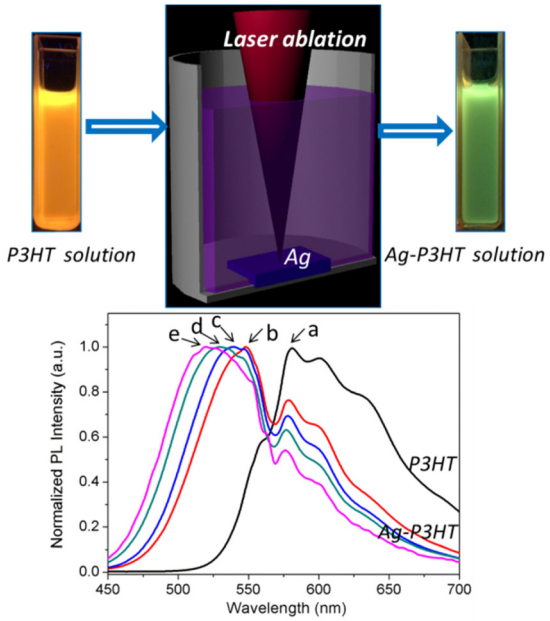

Fig. 1. Top: Illustration of experimental setup for fabrication of the Ag-P3HT nanocomposite by pulsed laser ablation. Ag target was immersed in a chloroform solution of P3HT. The photos show the fluorescence of chloroform solutions of P3HT (left) and Ag-P3HT (right) under UV illumination. Bottom: Wavelength tuning of PL for as-prepared Ag-P3HT a, emission maximum at 580 nm for P3HT; b-e, emission maxima at c.a. 550, 540, 530 and 520 nm respectively for Ag-P3HT.

As depicted in Fig. 1, a laser beam was focused on the surface of a silver target immersed in the P3HT solution. The central emission wavelength is 580 nm for a P3HT solution. After laser ablation for 15, 30, 40 and 50 min, the emission peak can be controllably tuned to c.a. 550, 540, 530 and 520 nm respectively. In the following section, we will present the experimental results to show that the solution is composed of new materials: nanocomposite of Ag and P3HT referred as Ag-P3HT. That is, the organic conjugated polymer P3HT was grafted onto Ag NPs via chemical links. In the following experiments, we report the sample with emission maximum at 530 nm as an example and exclude the possibility that the observed fluorescence change is due to Ag NP alone or degraded P3HT arising from the thermal effects of the high-power laser.

Optical Materials EXPRESS

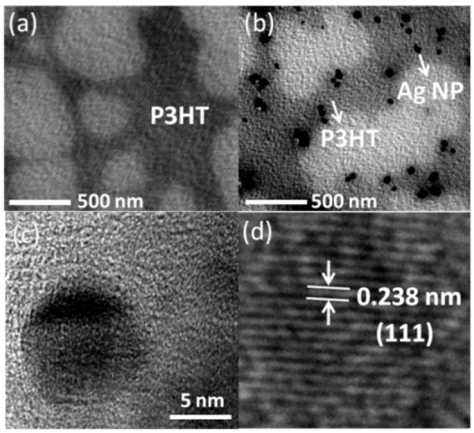

Fig. 2. (a) TEM image of pristine P3HT. TEM images of Ag-P3HT at low (b) and high magnification (c). (d) HRTEM image of Ag-P3HT.

Figure 2 shows the TEM images of pristine P3HT and as-prepared Ag-P3HT. In contrast to the neat P3HT with a porous film-like structure (Fig. 2(a)), silver NPs with sizes in a range from several to tens of nanometers were observed to be accrete and coexist within the P3HT matrix (Fig. 2(b) and 2(c)). Silver NPs formed in P3HT during the reaction process have been coated with an organic matrix of P3HT via chemical bond interactions. The well-dispersed Ag-P3HT nanocomposites have organic and inorganic phases at the molecular level. The HRTEM image in Fig. 2(d) provides typical nano-structural details of the as-prepared Ag-P3HT nanocomposite. The region in Fig. 2(d) with a lattice-fringe distance of 0.238 nm could be indexed with reference to the Ag (111) plane structures of the fcc silver crystal (JCPDS 04-0783).

Chemical binding in Ag-P3HT characterized by ^{1}H NMR, FTIR and XPS

^{1}H NMR spectroscopy was performed in order to elucidate unambiguously how P3HT is chemically bonded to Ag NP. Figure 3 exhibits the ^{1}H NMR (300MHz) spectra of P3HT and Ag-P3HT in the solvent $CDCl_3$. The peak at 7.26 ppm in both spectra for pristine P3HT and Ag-P3HT composite is from $CDCl_3$. The chemical shifts are 6.98 (s, 1H), 3.27 – 2.26 (m, 2H), 2.22 – 1.06 (m, 8H), 0.91 (t, J = 6.8 Hz, 3H) for pristine P3HT and 7.07 (s, 0.34H), 2.77 (d, J = 48.8 Hz, 2H), 1.38 (dd, J = 66.7, 49.4 Hz, 8H), 0.88 (t, J = 6.2 Hz, 3H) for Ag-P3HT. The peak at 6.98 and 7.07 ppm in each sample is attributed to protons on the thiophene ring moiety. The ratio intensity at ~7 ppm decreases from 1 for pristine P3HT to 0.34 for Ag-P3HT nanocomposite which was fabricated by laser ablation of 40 min, which indicates about 66% of hydrogen atoms on the thiophene rings in P3HT chains are replaced. When ablated for 50 min, the as-prepared Ag-P3HT has even smaller peak intensity at 7.07 ppm, i.e. 0.25. It implies that more hydrogen atoms are replaced by Ag NPs as the ablation duration increases, which is probably correlated with the blueshift of PL maximum. The alkyl proton signals are always observed to be in a quantitative ratio of 2:8:3, demonstrating the hydrogen atoms on the hexyl side chain are chemically unaffected. However, the three groups of hexyl proton peaks all become apparently wider. It may be associated with the formation of a chemical bond. Carbon(4) serves as a metal binding site and the chemical link was formed between thiophene rings and Ag NPs [17]. It is a C-H σ-bond metathesis process. P3HT chains bind to and cap the surface of Ag NPs.

Optical Materials EXPRESS

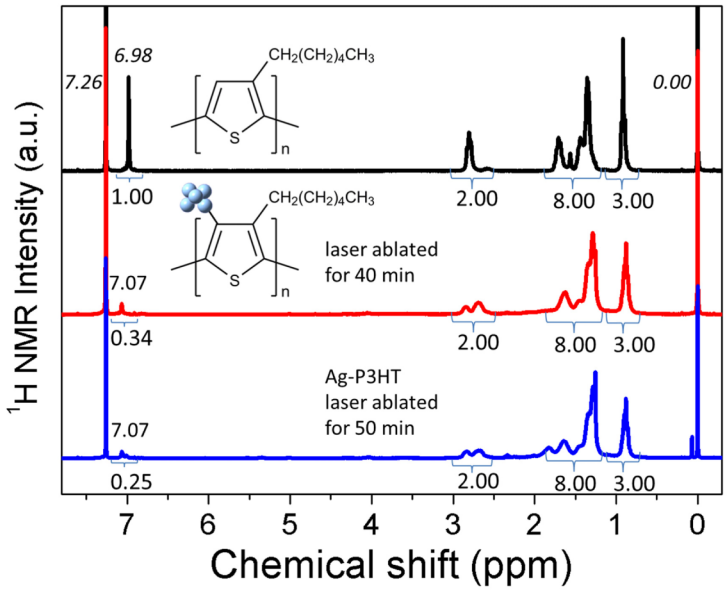

Fig. 3. ^{1}H NMR (300 MHz, $CDCl_3$) spectra of pristine P3HT (first row) and Ag-P3HT which was fabricated by laser ablation for 40 (second row) and 50 (third row) min. The top inset is the molecular structure of P3HT. The bottom inset is a schematic representation of the grafting position of P3HT to Ag NPs.

Silver NPs chemically linked to the thiophene carbon(4) influence other bonding properties of the thiophene rings, which can be revealed by FTIR spectra (see Fig. 4(a)). All the IR absorption bands of the thiophene ring are located between 400 and 2000 cm^{-1}. The spectrum of pristine P3HT show the following characteristic bands: 822 cm^{-1} (out-of-plane C–H vibration in the thiophene ring), 1087 cm^{-1} (C–S stretching in the thiophene ring), 1375 cm^{-1} (methyl bending), 1458 cm^{-1} (aromatic C = C symmetric stretching), 1510cm^{-1} (aromatic C = C asymmetric stretching) [18]. For Ag-P3HT, the intensity of the bands at 822, 1458 and 1510 cm^{-1} is reduced considerably but not the band 1087 at cm^{-1}. This indicates there is strong interaction between P3HT and the metal atoms. The C-S bond is the furthest away from the Ag NPs and hence is least affected. FTIR validates the NMR results that Ag NPs are chemically bonded to carbon(4) of the thiophene rings of P3HT.

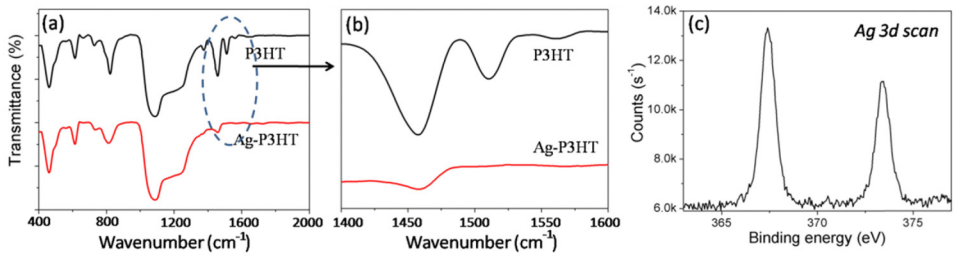

Fig. 4. (a) FTIR spectra of pristine P3HT and Ag-P3HT. (b) An expanded view of the FTIR data in the region 1400-1600 cm^{-1}. (c) XPS spectra for $3d_{5/2}$ and $3d_{3/2}$ Ag bands in Ag-P3HT.

The intensity ratio between the symmetric C = C stretching peak at 1458 cm^{-1} and the asymmetric stretching peak at 1510 cm^{-1} as displayed in Fig. 4(b) is indicative of the conjugation length of the P3HT polymer chain according to Chen et al [19]. Longer conjugation length in the polymer backbone results in a smaller I_{sym}/I_{asym} ratio. While the ratio is only 2 for pristine P3HT [16], it is 10.34 for Ag-P3HT, which suggests the conjugation

Optical Materials EXPRESS

length is decreased in the chemically-linked Ag-P3HT nanocomposite. The conjugation length is related to the luminescent properties of P3HT derivatives [20]. It is consistent with the variation in photoluminescence shown later in Fig. 5.

X-ray photoelectron spectroscopy (XPS) is used to confirm the valence state of silver in Ag-P3HT. Two bands are observed at 367.4 and 373.4 eV, corresponding to the binding energies of Ag $3d_{5/2}$ and Ag $3d_{3/2}$ respectively (Fig. 4(c)), which are attributed to Ag(I) in the nanocomposite of P3HT and Ag NP. It is different from the $Ag3d_{5/2}$ peak centered at 368.2–368.3 eV for the metallic Ag(0) [21]. Thus silver does not exist as Ag(0) in Ag-P3HT, but is chemically-tethered to P3HT in the Ag(I) state. This is consistent with Ag NP replacing H in the C-H σ-bond of thiophene in the metathesis process. The bond -C-S-Ag reported in previous studies [22] which corresponds to a peak at 161.8 eV was not observed in the as-prepared Ag-P3HT. This is in good qualitative agreement with the FTIR result that C-S bond was not influenced in the chemical reaction.

Luminescent properties of Ag-P3HT

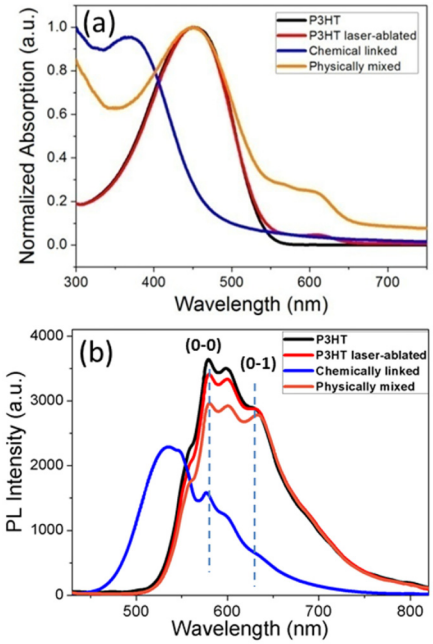

Fig. 5. Steady-state absorption (a) and PL (b) spectra of the solution of pristine P3HT, laser-ablated P3HT, chemically-linked Ag-P3HT nanocomposite, and physically mixed Ag NP/P3HT.

The absorption and emission were investigated for pristine P3HT, the as-prepared Ag-P3HT, as well as laser-ablated P3HT and physically mixed Ag NP/P3HT (see Fig. 5). To ensure the fluorescence changes do not arise from Ag NP or degraded P3HT due to the thermal effect of the high-power laser, P3HT and the Ag target were separately ablated in chloroform by the laser. The solution of Ag NP is not luminescent. This solution was afterwards physically mixed with P3HT. P3HT was ablated for the same time duration as Ag-P3HT. The laser-ablated P3HT is stable and the fluorescence spectrum remained unaltered. Hence, it may be concluded that the PL at 530 nm originates from Ag-P3HT and not from thermal degradation of P3HT or Ag NPs. Some research groups reported silver nanoclusters with diameters smaller than 2 nm are luminescent and their fluorescence maximum resides around 680 nm [16,23,24]. Since it was not observed in the PL spectra, we conclude that the luminescent Ag

Optical Materials EXPRESS

nanoclusters were not formed. P3HT chains grafted to Ag NP serve as a stabilizer to weaken the aggregations of Ag NPs.

The absorption spectra of the pristine P3HT in chloroform exhibited a maximum centered at 452 nm (2.74 eV), arising from the characteristic π-π* transition. This feature does not occur in the chemically-linked nanocomposite Ag-P3HT whose absorption is blueshifted to 370 nm. According to $(\alpha h\nu)^2 = A(h\nu - E_g)$ where α is the absorption coefficient and h*ν* is the photon energy [25], the bandgap Eg is 2.30 eV for pristine P3HT, in good agreement with literature values [14], and is 2.70 eV for Ag-P3HT. The absorption spectrum of laser-ablated P3HT almost coincides with that of pristine P3HT, except for a minor discrepancy in the long wavelength region 550-650 nm. This may be attributed to torsional defects of the thiophene ring chains produced in the ablation. The physically mixed sample still maintains the specific features at 452 nm and exhibits significant absorption below 400 nm due to the existence of Ag NPs.

In the emission spectra, pristine P3HT, laser-ablated P3HT and physically mixed P3HT and Ag NPs all show characteristic peaks at 580 nm (2.14 eV) and 633 nm (1.96 eV), nominally regarded as 0-0 and 0-1 features and attributed to the emission of intrachain excitons obeying the Franck–Condon principle. The difference in energy between the peak and shoulder emission is ~0.18 eV and can be ascribed to stretching vibration energy of the C = C bond in the polymer [26]. H-type (face-to-face) and J-type (head-to-tail) aggregates in the regio-regular P3HT films have been proposed [27]. In H aggregate systems, 0-0 electronic transitions between the ground state and the lowest energy level of the vibronic excited state are forbidden by symmetry, giving rise to a much larger 0-1 intensity than the 0-0 sideband. The intensity ratio $I_{0\text{-}1}/I_{0\text{-}0}$ increases as P3HT is ablated or physically mixed with Ag NPs, indicating the component ratio of the two aggregate types H-type/J-type gets larger. P3HT chains undergoing laser ablation may break to form shorter ones with lower molecule mass which prefer H aggregate. As to the case of physically mixed samples, the larger intensity ratio $I_{0\text{-}1}/I_{0\text{-}0}$ can be explained by the enhanced interchain interactions between neighboring P3HT chains which are physically adsorbed to Ag NPs [28].

The chemically bonded sample exhibited essentially different behavior, i.e. the main emission peak is blueshifted to 530 nm. Substituents such as Ag NPs affect the wavelength of emission as steric interactions can produce out-of-plane twisting of the polymer backbone [28]. The planarity of the conjugated polymer system is reduced in Ag-P3HT. Hence the effective conjugation length is decreased which localizes the wave function of excitons to a greater extent and therefore increases the bandgap [29]. The wavelength of the fluorescence maximum blueshifts with longer ablation time because more Ag-C bonds are formed and therefore increasingly change the conformation/planarity of the polymer. Ag-P3HT has a more coil-like conformation that leads to a more difficult planarization process, corresponding to the smaller $I_{0\text{-}1}/I_{0\text{-}0}$. The π-π stacking of thiophene rings and associated electronic transitions serve as the primary origins of fluorescence in P3HT and its derivatives. Therefore, the structural changes of thiophene rings induce a notable blueshift in absorption and photoluminescence peaks (see Fig. 5) of the samples in our study.

Optical Materials EXPRESS

Photophysical characterizations of Ag-P3HT

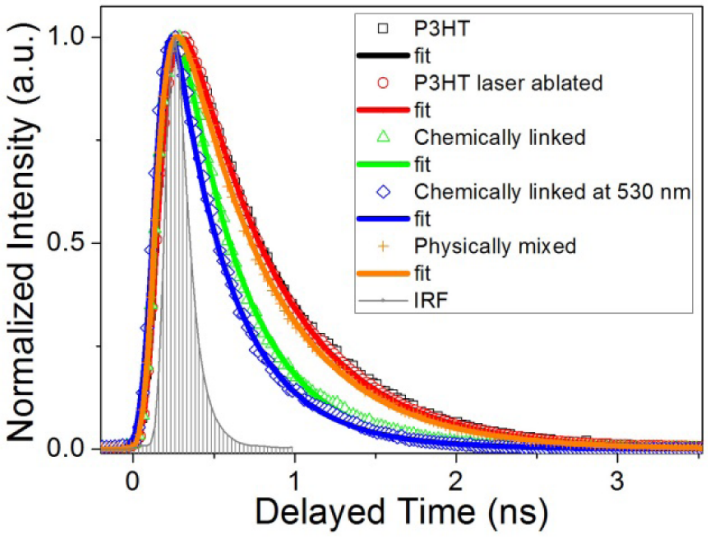

Fig. 6. Normalized time-resolved fluorescence decay profiles (TCSPC) of pristine P3HT and Ag-P3HT in chloroform solution. The grey area denotes the instrument response function (IRF).

To gain an insight into the charge transfer dynamics in Ag and P3HT nanocomposites, time-resolved fluorescence measurements were performed using a time-correlated single-photon-counting (TCSPC) methodology on four samples in chloroform solutions, (1) pristine P3HT, (2) laser-ablated P3HT, (3) physically mixed Ag/P3HT, and (4) chemically linked Ag-P3HT (Fig. 6). Physically mixed samples and laser-ablated P3HT were examined to unravel the exact origins of the photophysical behaviors. The excitation wavelength was fixed at 400 nm and fluorescence decay was detected at 580 nm, the P3HT emission peak, in all samples and also at 530 nm, the Ag-P3HT emission peak, for Sample 4. The obtained fluorescence decay curves were well-fitted by a single-exponential decay equation. The fitted data are listed in Table 1. The fluorescence lifetime is 616 ps for pristine P3HT and decreased slightly to 570 ps after laser ablation. It is tentatively suggested that P3HT chains are thermally broken into shorter ones in the ablation process, thus favoring interchain interactions which assist exciton dissociation [26]. The physical mixtures Ag/P3HT also show a small decrease in fluorescence lifetime to 562 ps, due to the limited interfacial contact and strong phase segregation of the two components. The chemically-bonded Ag-P3HT, however, exhibited a much faster decay lifetime of 358 ps which is attributed to the relaxation of singlet-state excitons [30]. Unlike the physically mixed Ag/P3HT, in Ag-P3HT metal NPs and P3HT chains are held in proximity via the stable chemical bond, facilitating the dissociation of excitons and charge transfer [31]. This is similar to the processes in a copolymer [32], except that the separate phase domain of Ag-P3HT is much larger than the one in a copolymer. Interchain interactions associated with shorter decay times relative to the intrachain counterpart are enhanced due to the neighboring P3HT chains that are chemically anchored to a same silver NP [16]. Nevertheless, it needs to be stressed that the above descriptions are just qualitative analysis on the chemically-linked Ag-P3HT structure. The detailed quantitative results, such as the exact number of polymer chains associated with each Ag NP, and the related mechanism by which the ablation process results in bond formation between Ag NPs and P3HT, *etc.* are still not exactly clear and remain to be explored.

Optical Materials EXPRESS

Table 1. Fit parameters for the fluorescence decays shown in Fig. 6. (All the samples were dissolved in chloroform and excited at 400 nm.)[a]

Solution samples	Detection wavelength (nm)	Fitted time τ (ps)
P3HT	580	616
P3HT ablated	580	570
Physical mixtures	580	562
Chemically-linked Ag-P3HT	580	412
	530	358

[a]Fluorescence decay curves are fitted to $I(t) = Ae^{-t/\tau}$

In accordance with the steady-state emission spectra, Ag-P3HT has a more coil-like conformation and the polymer chains in Ag-P3HT are twisted with more torsional defects. In this case the relaxation of excitons might be expected to be slower than that in pristine P3HT. However, the decay time was observed to be much smaller for Ag-P3HT than for P3HT. The shorter decay time can possibly be associated with the energy transfer from the excited state of P3HT to the surface plasmon resonance (SPR) state of silver NPs [33], in addition to the above mentioned interchain interactions and proximity due to the linking chemical bond [30,31].

In organic polymeric semiconductor materials, e.g. P3HT in this work, excitons usually recombine to emit fluorescence or dissociate at interfaces to generate free holes and electrons. In an ideal scenario, there is no interfacial site in pristine P3HT and excitons can be expected to recombine. Exciton dissociation in Ag-P3HT leads to the quenching of luminescence (Fig. 5(b)) and a faster fluorescence decay (Fig. 6). The efficiency of formation of free charge carriers in Ag-P3HT can be derived from the fitted fluorescence decay parameters using [34]:

$$\Phi_{\text{freecharge}} \approx 1 - \frac{\tau_{\text{Ag-P3HT}}}{\tau_{\text{P3HT}}}$$

where $\tau_{\text{Ag-P3HT}}$ and τ_{P3HT} are the fluorescence lifetimes of Ag-P3HT and pristine P3HT respectively. Therefore, for Ag-P3HT, $\Phi_{\text{freecharge}} = 0.4$, that is, 40% of excitons dissociate at interfaces and generate free charge pairs. The rate of change of exciton population can be described according to [34]

$$\frac{dN(t)}{dt} = -(k_{FL}(t) + k_{diss}(t))N(t)$$

where N(t) is the population of excitons, k_{FL} is the decay rate of exciton population due to recombination leading to fluorescence, and k_{diss} the decay rate of exciton population due to the dissociation at interfaces towards free holes and electrons. This equation can be analytically solved to be $N(t) = N(t=0)e^{-(k_{FL}(t)+k_{diss}(t))t}$. In the equation [35] $k_{diss}\tau = 4\pi cDR\left(1 + R/\sqrt{\pi Dt}\right)$, the coefficient k_{diss} depends on the concentration of interfacial contact sites c, the exciton diffusion coefficient D and R the distance of closest approach, beyond which excitons tend to be separated rather than recombine. For pristine P3HT, c is approximately 0, hence we have $N(t) = N(t=0)e^{-k_{FL}t}$ because k_{diss} is 0 for P3HT. For chemically-bonded Ag-P3HT and physically-mixed Ag/P3HT, $N(t) = N(t=0)e^{-(k_{FL}+k_{diss})t}$. The calculation based on the kinetic fluorescence properties gives $k_{dissAg-P3HT} = \tau_{P3HT}/\tau_{Ag-P3HT} - 1 = 0.7$ and $k_{dissAg/P3HT} = \tau_{P3HT}/\tau_{Ag/P3HT} - 1 = 0.09$ if normalized to k_{FL} as 1. The population of exciton decays at a rate which is 700% larger in the

Optical Materials EXPRESS

complex nanocomposite than in physical mixtures, implying the interfacial contact, exciton diffusion and finally the charge transfer and exciton separation efficiency is greatly enhanced due to the presence of the metal-thiophene chemical bond.

The conjugated polymer P3HT shows strong fluorescence centered at 580 nm. When the metal atom assemblies are introduced into the thiophene ring moieties, the luminescence of P3HT is altered. Carbon(4) of the thiophene ring is the metal binding site. Our results indicate a novel conjugation method of metal-polymer complexes by laser ablation, without any need of catalyst, surfactant or hydrothermal treatment, providing a green, low-cost and convenient synthesis technique. It paves the way to controllably adjusting the absorption and emission of organic materials through chemically tethering diverse categories of metal atom assemblies by this facile synthesis strategy. The method has great potential for the fabrication of various metal-organic compounds for applications in full-color OLED, photovoltaics and bioimaging etc.

4. Conclusion

In summary, novel Ag-P3HT organic-metal nanocomposites have been successfully synthesized by laser ablation. The structures of the as-prepared Ag-P3HT were characterized by NMR, FTIR and XPS spectroscopy. Steady-state absorption and emission spectra are significantly blueshifted for Ag-P3HT with respect to pristine P3HT, confirming the formation of chemical bonds between P3HT and silver NPs. The fluorescence wavelength can be tuned by controlling the ablation durations. Time-resolved fluorescence spectra of chemically bonded Ag-P3HT show a decay time of 358 ps, much smaller than 616 ps in pristine P3HT or 562 ps in physically mixed Ag/P3HT. This specific luminescence property is due to the metal NPs and P3HT chains being held in proximity via the stable chemical bond, facilitating the dissociation of excitons and charge transfer. This feature, together with enhanced interchain interactions and the SPR effect of Ag, significantly improves the generation efficiency of free charge carriers in the chemically-bonded nanocomposite. Our work provides an unconventional way to achieve conjugation of metal and organic polymers, pointing to a possibility to control the emission of organic materials through chemically tethering diverse categories of metal atom assemblies for potential applications in full-color OLED, photovoltaics and bioimaging.

Funding

National Natural Science Foundation of China (No. 11404190, 11575102, 11574181); Education Ministry of China (No. 20120131120006); Fundamental Research Funds of Shandong University (No. 2015JC007); “National Young 1000 Talents” Program of China.